

Characteristics of Black Carbon Aerosol at an Educational Site in Southern India

R. M. Rajeshkumar*, B. Vijay Bhaskar, K. Muthuchelian

*Department of Bioenergy, School of Energy,
Environment and Natural Resources, Madurai Kamaraj University, India*

*Corresponding Author: rmrk246@gmail.com
Received: May 28, 2018; Accepted: September 12, 2018

Abstract

Black carbon (BC) aerosol formed from incomplete combustion of fossil fuel and biomass combustion is collected at an educational institute, Madurai Kamaraj University, Madurai located in Southern India. The sampling is done using an Aethalometer (AE-31) from January to March (2015 to 2017) to study the effect of meteorological parameters and anthropogenic activities during the transition from winter to summer. BC identified from a variety of sources showed strong diurnal variation with two peaks, first one at early morning hours and the other one at evening hours, but this peak timings varied with the seasons. It is observed that biomass combustion and tobacco smoke at the study site dominates other sources. Raman spectral analysis showed strong organic source peak.

Keywords: Black carbon; Educational Institution; Tobacco smoke; Raman Spectrum

1. Introduction

Aerosols are quite ubiquitous; airborne particles from volcanic eruptions, cigarette smoke, smoke from power generation, and salt particles formed from ocean spray (Pramod *et al.* 2011). Incomplete combustion of fossil fuel, biofuel, and biomass result in the formation of organic carbon (OC), and black carbon (BC) aerosols (Ramachandran and Rajesh, 2017). BC is one among the most important constituent of ambient particulate matter and it remains inert in the atmosphere based on its predominant sub-micron size and chemical structure. Globally emitted BC aerosols from anthropogenic activities were estimated from bottom-up approaches, and are reported to be

7500 Gg/year, but with a large uncertainty range of 2000–29000 Gg/year (Bond *et al.*, 2013 and Kumar *et al.*, 2015). BC aerosols accumulate in the tropospheric region and disturb the radiative balance with its strong solar radiation absorption characteristics (Bond *et al.*, 2013, Jacobson, 2014). Due to its efficient light absorbing nature, BC exerts a positive direct radiative forcing on Earth's climate between +0.08–1.27 W/m² (Bond *et al.*, 2013). BC aerosols stay in the atmosphere for a very short duration (few days to weeks). During the atmospheric process, freshly formed BC aerosols are usually hydrophobic, while aged particles turn into hygroscopic with the coating of other pollutants. According to Bond and Bergstrom (2006), mass absorption cross-section of freshly formed uncoated BC

ranges between (4 to 8) m^2/g whereas due to the pollutants coated BC results in the increase of mass absorption cross-section. Different source coating results in different wavelength absorption (Bond and Bergstrom, 2006). A hematite form of iron oxides which is an important composition of aerosols absorb visible light at wavelengths $< 600\text{nm}$ (Sokolik and Toon, 1999; Yang *et al.*, 2009). Studies conducted by Gadhavi and Jayaraman (2010) and Tiwari *et al.* (2014) during winter using aethalometer found that 20–40% and ~6% of the BC originates from biomass combustion measured at 370 nm. The probable major source of BC can be identified by the value of the absorption angstrom exponent (AAE).

BC is a major part of particulate matter, with a size less than 2.5 microns ($\text{PM}_{2.5}$) (Paliwal *et al.*, 2016). Raman Spectroscopic analysis of particulate matters (PM) gives information about its composition. The Raman spectroscopic analysis on PM depends on the vibrational modes exerted by them (Ivleva *et al.*, 2007). The scattered light produced from PM, which depends upon the lattice arrangement shows specific wavelength shifts. These shifts can be used to identify different composition. The Graphitic (G) band and Distorted (D) band produced by carbonaceous particles reveals information about the type and sources. According to Ivleva *et al.*, 2007, the shapes of the bands helped to understand about the humic

like substance from diesel soot. Temperature history and reactivity of the soot samples also can be determined from the bands (Carrara *et al.*, 2009). Mertes *et al.* (2004) used quartz fiber filters for capturing Elemental carbon (EC) aerosol, which is a refractory constituent. Quantitative Raman spectroscopy study on EC showed Raman intensities between 510 cm^{-1} and 1736 cm^{-1} . EC exhibits near similar trends in seasonal variations as BC aerosols. The absorption coefficient of EC is the essential input parameter for direct radiative forcing calculation.

In this experimental study, continuous measurement of black carbon aerosols in relationship with the meteorological parameters is conducted at a semi-arid site. The study is carried down from 2015 to 2017 to understand the light attenuation and absorption properties of aerosols during the transition between winter to summer months (January to March). The boundary layer dynamics, sunrise and sunset timings, meteorological conditions and black carbon concentration vary significantly during the transition between the winter and the summer months at the study site. This study helps to comprehend the optical properties and identify the major sources of BC during winter and post winter month.

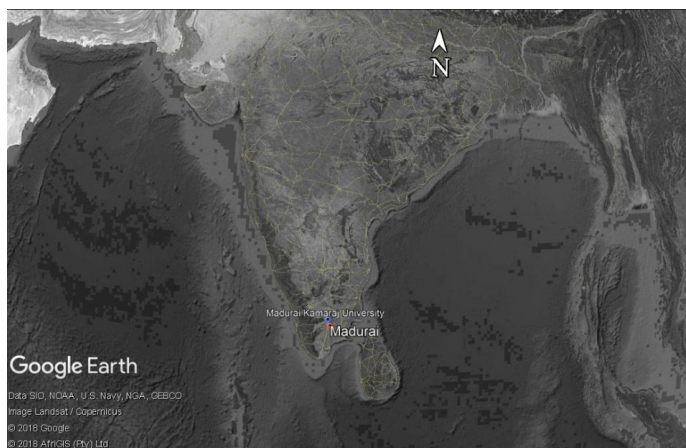


Figure 1. Google Earth imagery showing the study site Madurai Kamaraj University (9.94° N , 78.01° E) located at an semi-arid location in Southern India

2. Materials and Methods

2.1. Study Site

Madurai (9°91'N, 78°54'E), located 130 m above mean sea level is one among the emerging mega city. It is the second largest and one among the most densely populated city in the southern India covering a surface area of 52.8 km² and a population of 3.2 million in 2011 while it was 0.25 million in 2001, excluding the ~0.1 million floating population. The sampling was carried down at Highway cum vegetation covered rural location in Madurai (Madurai Kamaraj University), located at the foothills of Nagamalai and adjacent to the Madurai-Theni National Highway NH-85 and is on the outskirts of the nearest populated city (about 12.8 km) (Figure 1). During sampling the outdoor air temperature ranged from 22 to 31 °C with a relative humidity range of 62–90%. Windspeed are generally <5 m/sec and frequently from the northeast and southwest directions (Table 1).

2.2 Instrumentation

Black carbon mass concentration is measured using seven-wavelength (370, 470, 520, 590, 660, 880 and 950 nm) based AE-31 model Aethalometer (Magee Scientific Corporation, USA). The aerosols are collected using an inlet tube and a pump which operates at a stable airflow rate about 3 L/min with a time interval of 5 min. Aethalometer depends on filter based technique to measure the variability in light attenuation due to particles deposited onto a filter.

In the aethalometer, the measured attenuation is linearly proportional to the BC mass deposit. Hence, by using the wavelength dependent calibration factors, the light attenuation

absorption coefficient is converted into BC mass concentration (Hansen, 2005 and Yang *et al.*, 2009). The babs in relation to the change in attenuation are given below as:

$$b_{abs}(\lambda) = \frac{1}{CR(ATN)} \times \frac{\Delta ATN(\lambda)}{\Delta t} \times \frac{A}{Q} \quad \text{Eq.1}$$

where, b_{abs} is the absorption coefficient, ΔATN , the ratio of the intensities of incoming light to the remaining light after passing through an optical path, for sensing beam and the reference beam respectively, $s_{an} = \frac{14625}{\lambda}$, the specific attenuation cross section; A, the spot area and Q, the volume of air passed through the filter. The parameters C and R (ATN) were correction factors for minimizing the uncertainty in the readings associated with Aethalometer. The light absorption measured at 880 nm is considered to represent the effect of BC (Bodhaine, 1995) as there were no other major aerosol species which exhibits an absorption at that wavelength. The absorption angstrom exponent (AAE) is a measure of spectral dependence of aerosol absorption (Park *et al.*, 2006; Sandradewi *et al.*, 2008; Ajtai *et al.*, 2011; and Srivastava *et al.*, 2012).

$$b_{abs}(\lambda) = \beta \lambda^{-AAE} \quad \text{Eq.2}$$

where, β is the particle loading, a constant and λ is the wavelength. Using the power law equation (2) and by performing a linear regression of $\ln(b_{abs})$ and $\ln(\lambda)$ (Kirchstetter *et al.*, 2004) AAE is calculated. BC concentration measured using ATN at 880 nm channel with a σ_{atn} value of 16.6 m²/g is considered standard (Nair *et al.*, 2007; Beegum *et al.*, 2009; Gadhavi and Jayaraman, 2010; Kumar *et al.*, 2011; Dumka *et al.*, 2013). The calculation of Delta-C suggest-

Table 1. Monthly mean values of Air temperature, Windspeed, Relative Humidity, Sunrise, Sunset timings and Ventilation coefficient at the study site during the study period.

Months	Air temperature (°C)	Windspeed (m/sec)	Relative Humidity (%)	VC (m ² /sec)	Sunrise time (LT)	Sunset time (LT)
January	27 ± 1	3.3 ± 1.2	71	3.42	6:34	18:07
February	28 ± 2	2.7 ± 3.0	62	3.10	6:32	18:22
March	31 ± 1	1.9 ± 0.8	65	2.04	6:15	18:28

ed by Allen *et al.* (2004) serve as an indicator of wood burning particles, but not a direct quantitative measurement of mass concentrations.

$$\Delta C = BC_{(370nm)} - BC_{(880nm)}$$

Thermo electrically cooled charge coupled device based HORIBA Jobin Yvon LabRam HR 800 spectrometer is used to study the micro-Raman spectrum. A 1800 grooves mm^{-1} and 2400 grooves mm^{-1} holographic grating is used to equip the spectrograph. The power of He-Ne (633 nm) and mixed gas laser line (488 nm) is 17 and 55 mW respectively. The size of the laser spot on the sample is approximately 1 μm in diameter. The collection time of the spectrum is 3 seconds and a 40X objective is used to focus and collect the scattered signal.

3. Results and Discussion

3.1 Diurnal variation of BC concentration

Continuous BC aerosol mass concentration sampling is carried out for 24 hours per day during the months January to March during the years 2015 to 2017 and their mean concentration values are calculated for those months using equation 1. The boundary layer dynamics, sunrise and sunset timings, meteorological conditions and black carbon concentration vary significantly during the transition between the winter and the summer months at the study site. Figure 2 shows the monthly mean diurnal variation of BC aerosols with vertical bars denoting the standard deviation. It is evident from the graph that for all the three months, sharp peaks are observed during the 6:00 to 9:00 hours and 19:00 to 22:00 hours. The BC concentration decrease gradually during noon hours and a stable BC mass concentration is observed.

The sunrise and sunset timings during January to March is shown in table 1. The time interval between sunrise and sunset is the length of the day (hours) and the remaining interval is the length of the night (hours) (Ramachandran and Rajesh, 2017). According to Ramachandran and Rajesh (2007), as a result of fumigation effect, during the early morning sunrise hours the first peak in diurnal BC mass concentration is observed. Early morning hour's solar heating

causes lifting of aerosol particles which are confined to the surface during the night hours. The early morning concentration peak timing varies with season, because the change in the sunrise timings during different seasons is directly proportional to the peak timings (Latha and Badarinath, 2005; Tripathi *et al.*, 2005; Safai *et al.*, 2007; Nair *et al.*, 2007). According to Ramachandran and Rajesh (2017), as a result of fully evolved boundary layer and increased solar radiation during the noon hours, there is a decreased BC concentration during those hours. Decrease in boundary layer height and increased cooking and other anthropogenic activities during the evening causes the second peak (19:00 to 22:00 hours).

BC aerosol concentration in the study site is analyzed using the absorption angstrom exponent (AAE) analysis (Equation 2). The AAE values showed that the values ranged from 0.9 to 1.8 with the average value of 1.2. According to Kirchstetter *et al.* 2004, and Herich *et al.* 2011, the values of AAE less than or equal to 1.0 indicates the dominance of fossil fuel burning and the value around 1.5 represents BC mixed with larger sized mineral dust particles, whereas the AAE for soot particles evolved from biomass combustion ranged from 1.5 to 3.0. As the study site is located away from the polluting urban environment, industrial and brick kiln sources impacts are very low. Therefore, the most common known sources emitted are from fossil fuel (ff) and biomass wood burning (wb) at the study site. An emission inventory was done for this study site based on the sources of BC concentration and from the study it was concluded that the two most dominating sources were biomass and fossil fuel combustion (Bhaskar *et al.*, 2018). Emissions from the brickkiln and forest fire were very low compared to the biomass and fossil fuel sources because the study site was completely isolated from such activities. Tobacco smoke emissions were included in the study.

Figure 3(a) show the diurnal variation with consistent changes in BC concentration contributed from fossil fuel sources (BC_{ff}) and wood burning sources (BC_{wb}). During the study period, BC_{ff} contributes in larger account to the BC throughout January with peak values during

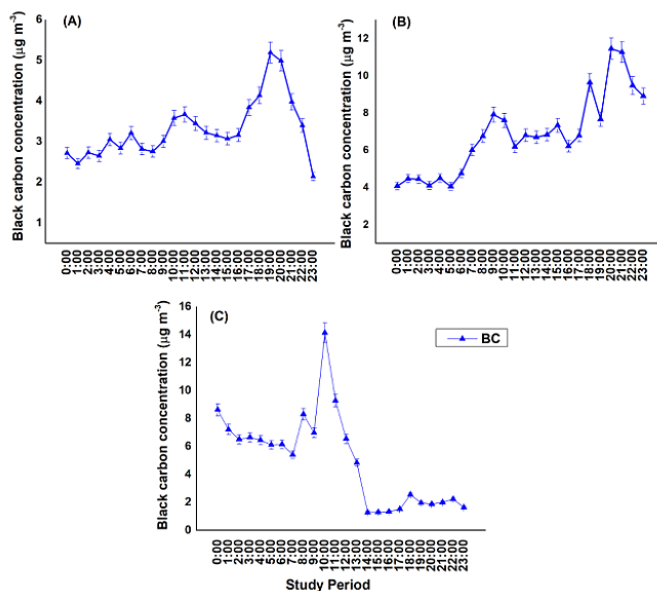


Figure 2. Hourly mean diurnal variation of BC concentration measured during the study period

late night hours extending up to the early morning hours. Figure 3(b) shows the percentage contribution of (BC_{ff}) and (BC_{wb}) during day and night hours. The percentage contribution of BC_{ff} during January is due to the increased flow of heavy tonnage vehicles (HTV) containing essentials for the Pongal, a local festival and also due to the increased population reaching university after the vacation days (extending from second week of December up to first week of January). The number of vehicles crossing the study site ranges from 1000 to 5000 per day during January, while the vehicular population range changes from 500 to 1000 per day during February and March. During February and March months biomass contribution BC_{wb} to the total BC is found higher during both morning and evening hours. The contribution of BC_{wb} is higher by a factor of 2–4 than BC_{ff} contributions. The percentage contribution of BC_{wb} is high during February, because of an increased usage of biomass combustion including the burning of crop residue (mostly sugarcane residue) (Bhaskar *et al.*, 2018) and the decreased flow of vehicles. The number of rainfall events during the study period plays a vital role in the decreased BC concentration compared during March, because the total number of rainfall

events in January and February combined is 21 while in March alone is 30 to 45 events per year. The rainfall events recorded in March is mostly during the daytime hours. A pronounced evening peak in BC_{wb} throughout the March was due to the significant and dominant wet biomass combustion activity, while during night to early morning hours lot of fossil fuel contribution is recorded.

To evaluate the dominance of BC_{wb} , Delta-C analysis is carried out and the results are plotted in Figure 4 and it shows a strong diurnal variation. According to Hopke *et al.* (2011), if wood combustion smoke is present then Delta-C values are positive, if not, then the values would be negative and the negative values might be from the filter between consecutive sampling, during which the desorption of UV absorbing semi-volatile organic species occurs. The changes Delta-C values during January are found to be negative in day and night hours indicating the dominance of BC_{ff} activities, while during February and March there is an increased positive Delta-C during day time. The gradual buildup of early morning Delta-C values during February month likely corresponded with an increase of residential wood burning emissions after sunrise.

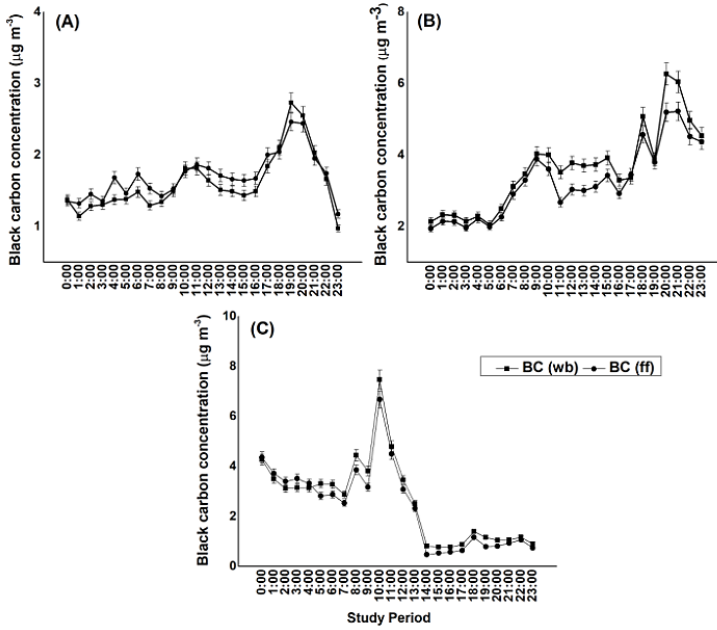


Figure 3(a). Hourly mean diurnal variation of BC concentration contributed from BC_{ff} and BC_{wb} (a) January (b) February and (c) March

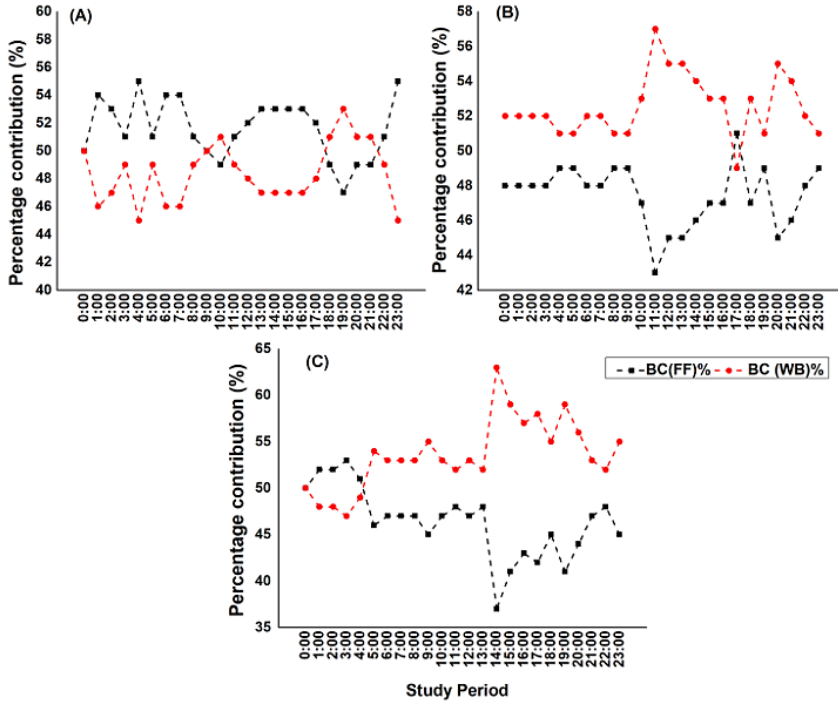


Figure 3(b). Mean percentage contribution of BC_{ff} and BC_{wb} to the total BC concentration (a) January (b) February and (c) March

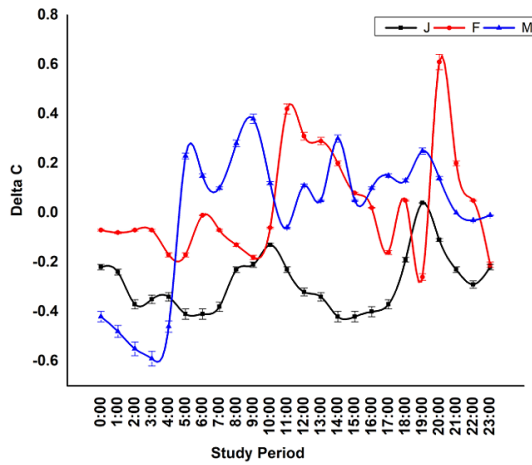


Figure 4. Delta-C analysis for the study period

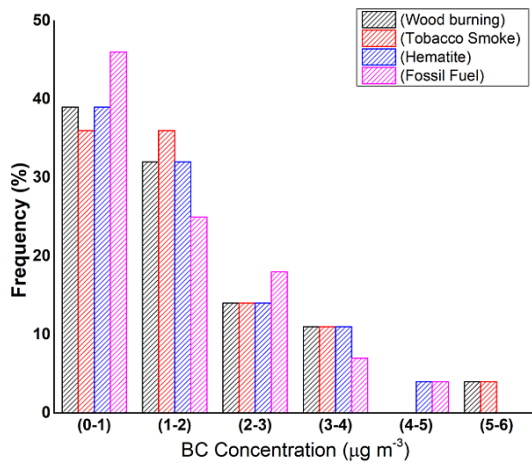


Figure 5(a). Frequency distribution (%) of BC concentration from different sources

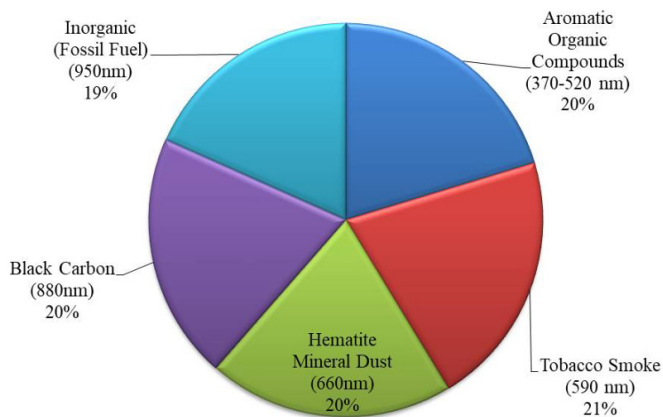


Figure 5(b). Pie chart showing the BC concentration from different sources measured at different wavelength

3.2 Contribution of different sources

Sources other than fossil fuel and biomass contributing to the total BC concentration which includes Tobacco smoke and Hematite mineral dusts are recorded at different wavelengths 590nm and 660nm, respectively using the aethalometer and analyzed. The preferences of wavelengths for such sources were obtained from the aethalometer manual (Hansen, 2005). During the study period the BC from different sources are classified and it ranged from (0.22 to 8.69) $\mu\text{g m}^{-3}$ and their frequency distribution based on the concentration is shown in figure 5(a). From the frequency distribution, higher concentration of BC $>5 \mu\text{g m}^{-3}$ are purely from wood combustion and tobacco smoke. Figure 5(b) shows the percentage distribution of BC from different sources. From the results it is observed that, at Madurai Kamaraj University the percentage contribution from tobacco smoke dominates over the other sources. Tobacco smoke contributes with a major share of 21%, 21% and 23% during the months of January, February and March respectively. Diurnal variation of BC tobacco smoke (BC_T) contribution to the total BC is analyzed and plotted (Figure 6). Table 2 shows the studies from other sites.

3.3 Molecular Analysis

This study is based upon the aerosol morphology, its light absorbing characteristics

and the nature of internally mixed soot particles (Liousse *et al.*, 1993; Bond and Bergstrom, 2006). The ability of BC aerosols to absorb light arises from the molecular structure which is characterized by the valence electrons in the π - orbitals. Small energy gaps between bonding and anti-bonding orbitals allows the BC aerosols to absorb visible light. Based on the Raman Spectrum (RS) mode analysis of Ivleva *et al.* (2007), G band occurrence at 1576 to 1585 cm^{-1} confirms the graphitic nature (hexagonal) of the observed samples, as black carbon aerosols are graphitic in nature and the occurrence of 1325 cm^{-1} shows the non-hexagonal structure that represents the organic substance present in the sample. For the samples collected during February and March the Raman intensity for D band is high, confirming the dominance of organic sources (Figure 7).

BC mass concentration of different anthropogenic sources, including fossil fuel (BC_{ff}), wood burning (BC_{wb}) and from other sources are investigated during the years 2015 to 2017 at an educational institution located in Southern India. Higher BC concentration is observed during winter (January-February) and first month of summer (March) when compared to other monsoon and post monsoon months at the study site. The major findings and results obtained from the study are summarized as follows:

Table 2. Black Carbon concentration over different study locations

Location	Location Type	Duration	BC ($\mu\text{g}/\text{m}^3$)	Reference
Mumbai	Urban, Industrial	January to March 1999	12.5	Venkatraman <i>et al.</i> (2005)
Hyderabad	Urban, Semi-arid	January to December 2003	10.0	Latha and Badrinath (2005)
Anantapur	Rural, Semi-arid	January to December 2010	5.05	Reddy <i>et al.</i> (2012)
Agartala, Tripura	Rural, Continental	September 2010 to September 2012	17.8	Guha <i>et al.</i> (2015)
Madurai	Urban, Semi-arid	January to March 2015 to 2017	1.62	This study

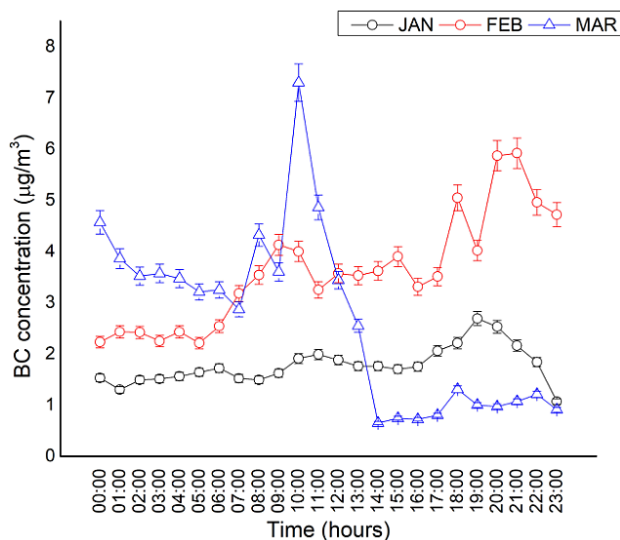


Figure 6. Hourly mean diurnal BC concentration during the study period.

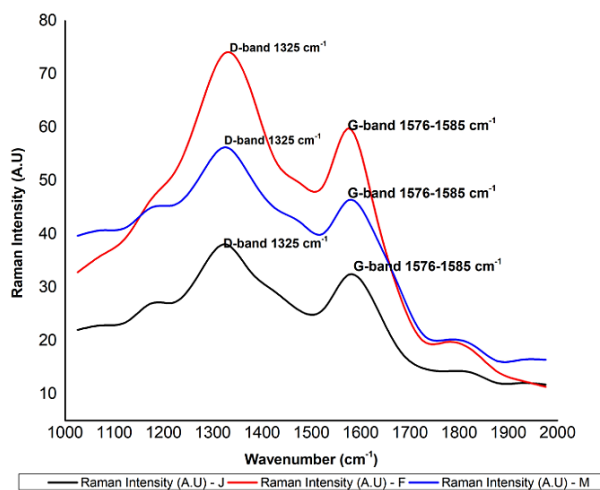


Figure 7. Raman spectral analysis of samples collected during the study period.

BC, exhibits a strong monthly variability with $8.69 \mu\text{g m}^{-3}$ during February and a low $0.22 \mu\text{g m}^{-3}$ during March. Higher BC during January and February arise due to shallow winter atmospheric boundary layer associated with low wind speeds, and significant increase in the amount of fossil fuel combustion and biomass burning, while lower BC concentration during March months are due to wet removal of aerosols and elevated boundary layer height.

Due to the diurnal changes in strength of BC emission sources and boundary layer height,

the BC mass concentrations exhibit strong diurnal variation. During the noon hours, the BC, BC_{ff} and BC_{wb} mass concentration values are high throughout the study period because of the fully evolved boundary layer and reduced anthropogenic activities. The contribution of BC_{wb} was higher by a factor of 2–4 than BC_{ff} and dominates throughout the day, which indicates persistent anthropogenic activities. In addition, contribution from tobacco smoke (BC_{ts}) at the study site dominates over the BC_{ff} and BC_{wb} contributions. Highest BC_{ts} (23%) and BC_{wb}

(22%) contribution is observed during March.

Using LabRam HR 800 system coupled with 325 nm excitation laser lines, the Raman mapping of sample was carried out. The Raman spectral analysis shows the domination of BC aerosols produced from biomass sources during the study period.

Acknowledgement

The authors are grateful to DST-SERB for providing fund and thank Madurai Kamaraj University for proving space to carry out this current research work.

Reference

- Ajtai T, Filep Á, Kecskeméti G, Hopp B, Bozók Z, Szabó G. Wavelength Dependent Mass-Specific Optical Absorption Coefficients of Laser Generated Coal Aerosols Determined from Multi-Wavelength Photoacoustic Measurements. *Applied Physics A* 2011; 103(4): 1165–1172.
- Allen GA, Babich P, Poirot RL. Evaluation of a new approach for real time assessment of wood smoke PM. *Proceedings of the Regional and Global Perspectives on Haze: Causes, Consequences and Controversies—Visibility Specialty Conference*, Asheville, North Carolina, A&WMA, Pittsburgh, PA. 2004.
- Beegum SN, KrishnaMoorthy K, SureshBabu S, Satheesh SK, Vinoj V, Badarinath KVS, Safai PD, Devara PCS, Singh S, Vinod, Dumka UC, Pant P. Spatial Distribution of Aerosol Black Carbon over India during Pre-monsoon Season. *Atmospheric Environment* 2009; 43(5): 1071–1078.
- Bhaskar VB, Rajeshkumar RM, and Muthuchelian K, An Emission Inventory-Based Study on Black Carbon Aerosols Produced During Biomass Burning. *Aerosol Science and Engineering* 2018; 2(3):141-152.
- Bodhaine BA. Aerosol absorption measurements at Barrow, Mauna Loa and the South Pole. *Journal of Geophysical Research* 1995; 100(D5): 8967–8975.
- Bond TC and Bergstrom RW. Light absorption by carbonaceous particles: An investigative review, *Aerosol Science and Technology* 2006; 40(1): 27–67.
- Bond TC, Doherty SJ, Fahey DW, Forster PM, Berntsen T, DeAngelo BJ, Flanner MG, Ghan S, Kärcher B, Koch D, Kinne S, Kondo Y, Quinn PK, Sarofim MC, et al. Bounding the role of black carbon in the climate system: A scientific assessment, *Journal of Geophysical Research.-Atmospheres* 2013; 118(11): 5380–5552, doi:10.1002/Jgrd.50171.
- Dumka UC, Manchanda RK, Sinha PR, Sreenivasan S, KrishnaMoorthy K, Suresh Babu S. Temporal variability and radiative impact of black carbon aerosol over tropical urban station Hyderabad. *Journal of Atmospheric and Solar-Terrestrial Physics*. 2013; 105-106: 81–90.
- Gadhavi H and Jayaraman A. Absorbing Aerosols: Contribution of Biomass Burning and Implications for Radiative Forcing. *Anales Geophysicae* 2010; 28(1): 103–111.
- Guha A, De BK, Dhar P, Banik T, Chakraborty M, Roy R, Choudhury A, Gogoi MM, Babu SS, Krishnamoorthy K. Seasonal Characteristics of Aerosol Black Carbon in Relation to Long Range Transport over Tripura in Northeast India. *Aerosol and Air Quality Research*, 2015; 15(3): 786–798
- Hansen ADA. <http://www.mageesci.com/book/Aethalometer-book-2005.07.03>. 2005
- Herich H, Hueglin C, and Buchmann B. A 2.5 year's source apportionment study of black carbon from wood burning and fossil fuel combustion at urban and rural sites in Switzerland. *Atmospheric Measurement Techniques* 2011; 4(7): 1409–1420. doi:10.5194/amt-4-1409-2011
- Wang Y, Hopke PK, Rattigan OV and Zhu Y. Characterization of ambient black carbon and wood burning particles in two urban areas. *Journal of Environmental Monitoring* 2011; 13(7): 1919-1926, DOI: 10.1039/c1em10117j
- Ivleva NP, McKeon U, Niessner R and Poschl U. Raman microspectroscopic analysis of size-resolved atmospheric aerosol particle samples collected with an elpi: Soot, hu-

- mic-like substances, and inorganic compounds. *Aerosol Science and Technology* 2007; 41(7): 655–671.
- Jacobson MZ. Effects of biomass burning on climate, accounting for heat and moisture fluxes, black and brown carbon, and cloud absorption effects. *Journal of Geophysical Research – Atmospheres* 2014;119(14):8980–9002. doi:10.1002/2014JD021861.
- Kirchstetter TW, Novakov T, Hobbs PV. Evidence that the spectral dependence of light absorption by aerosols is affected by organic carbon. *Journal of Geophysical Research - Atmospheres* 2004; 109(D21): D21208. doi:10.1029/2004JD004999
- Knauer M, Carrara M, Rothe D, Niessner R and Ivleva NP. Changes in structure and reactivity of soot during oxidation and gasification by oxygen, studied by micro-Raman spectroscopy and temperature programmed oxidation. *Aerosol Science and Technology* 2009; 43(1): 1–8.
- Kumar RK, Narasimhulu K, Balakrishnaiah G, Reddy BSK, Ramagopal K, Reddy RR, Satheesh SK, Krishnamoorthy K, Sureshbabu S. Characterization of Aerosol Black Carbon over a Tropical Semi-arid Region of Anantapur, India. *Atmospheric Research* 2011; 100(1): 12–27.
- Kumar R, Barth MC, Pfister GG, Nair VS, Ghude D, Ojha N. What controls the seasonal cycle of black carbon aerosols in India? *Journal of Geophysical Research-Atmospheres* 2015; 120: 7788–7812, doi:10.1002/2015JD023298.
- Latha KM and Badarinath KVS. Seasonal Variations of Black Carbon Aerosols and Total Aerosol Mass Concentrations over Urban Environment in India. *Atmospheric Environment* 2005; 39: 4129–4141.
- Lioussé C, Cachier H, Jennings G. Optical and Thermal Measurements of Black Carbon Contents Indifferent Environments: Variation of the Specific Attenuation Cross-section, Sigma (s). *Atmospheric Environment* 1993; 27(8): 1203–1211.
- Martes S, Dippel B, Schwarzenbock A. Quantification of graphitic carbon in atmospheric aerosol particles by Raman spectroscopy and first application for the determination of mass absorption efficiencies. *Journal of Aerosol Science*, 2004; 35(3): 347–361.
- Nair VS, Moorthy KK, Alappattu DP, Kunhikrishnan PK, Prabha SG, Nair R, Babu SS, Abish B, Satheesh SK, Tripathi SN, Niranjan K, Madhavan BL, Srikant V, Dutt CBS, Badarinath KVS, Reddy RR. Winter Time Aerosol Characteristics over the Indo-Gangetic Plane (IGP): Impacts of the Local Boundary Layer Processes and Long Range Transport. *Journal of Geophysical Research* 2007; 112:D13205.doi:10.1029/2006JD008099.
- Paliwall U, Sharma M and Burkhart JF. Monthly and spatially resolved black carbon emission inventory of India: uncertainty analysis, *Atmospheric chemistry and physics* 2016; 16(19): 12457-12476,https://doi.org/10.5194/acp-16-12457-2016.
- Park K, Chow JC, Watson JG, Trimble DL, Doraiswamy P, Park K, Arnott WP, Stroud KR, Bowers K, Bode R, Petzold A, Hansen AD. Comparison of Continuous and Filter-Based Carbon Measurements at the Fresno Supersite. *Journal of the Air & Waste Management Association* 2006; 56(4): 474–491.
- Kulkarni P, Baron PA, Willeke K. Introduction to Aerosol Characterization. *Aerosol Measurement: Principles, Techniques, and Applications*, Third Edition, Wiley Online Library. 2011.
- Ramachandran S, and Rajesh TA. Black carbon aerosol mass concentrations over Ahmedabad, an urban location in western India: comparison with urban sites in Asia, Europe, Canada, and the United States. *Journal of Geophysical Research* 2007;112(D6):D06211.doi:10.1029/2006JD007488
- Ramachandran S, and Rajesh TA. Characteristics and source apportionment of black carbon aerosols over an urban site. *Environmental Science and Pollution Research* 2017; 24(9): 8411-8424 DOI 10.1007/s11356-017-8453-3

- Reddy BSK, Kumar KR, Balakrishnaiah G, Ramagopal K, Reddy RR, Reddy LSS. Potential Source Regions Contributing to Seasonal Variation of Black Carbon Aerosols over Anantapur in Southeast India. *Aerosol and Air Quality Research*. 2012; 12(3): 344–358.
- Safai PD, Kewat S, Praveen PS, Rao PSP, Momin GA, Ali K, Devara PCS. Seasonal Variation of Black Carbon Aerosols over a Tropical Urban City of Pune, India. *Atmospheric Environment* 2007; 41(13): 2699–2709.
- Sandradewi J, Prevot ASH, Weingartner E, Schmidhauser R, Gysel M, Baltensperger U. A study of wood burning and traffic aerosols in an Alpine valley using a multi-wavelength Aethalometer. *Atmospheric Environment* 2008; 42(1):101–112.
- Sokolik IN and Toon OB. Incorporation of mineralogical composition into models of the radiative properties of mineral aerosol from UV to IR wavelengths. *Journal of Geophysical Research*, 1999; 104(D8): 9423-9444.
- Srivastava AK, Singh S, Pant P, Dumka UC. Characteristics of black carbon over Delhi and Manora Peak—a comparative study. *Atmos Sci Lett*. 2012;13(3):223–230. doi:10.1002/asl.386
- Tiwari S, Pipal AS, Srivastava AK, Bisht DS, Pandithurai G. Determination of wood burning and fossil fuel contribution of black carbon at Delhi, India using aerosol light absorption technique. *Environmental Science and Pollution Research* 2014; 22(4): 2846-2855
- Tripathi SN, Dey S, Tare V, Satheesh SK. Aerosol black carbon radiative forcing at an industrial city in northern India. *Geophysical Research Letters*. 2005; 32(8): Lo8802, doi:10.1029/ 2005GLO22515.
- Venkataraman C, Habib G, Eiguren-Fernandez A, Miguel AH, Friedlander SK. Residential biofuels in South Asia: carbonaceous aerosol emissions and climate impacts. *Science*. 2005; 307(5714): 1454–1456.
- Yang M, Howell SG, Zhuang J, and Huebert BJ. Attribution of aerosol light absorption to black carbon, brown carbon, and dust in China – interpretations of atmospheric measurements during EAST-ATRE. *Atmospheric Chemistry and Physics*, 2009; 9(6): 2035–2050.